Isotropic 3D Imaging Over Large Volumes with Axially Swept Light-Sheet Microscopy

Kevin M. Dean[1,2] **and Reto Fiolka**[2]

Affiliation:
[1]**Lyda Hill Department of Bioinformatics, University of Texas Southwestern Medical Center, Dallas, TX.**
[2]**Department of Cell Biology, University of Texas Southwestern Medical Center, Dallas, TX.**

Fluorescence microscopy, because of its high spatiotemporal resolution (Ahrens *et al.*, 2013), single-molecule sensitivity (Van Engelenburg *et al.*, 2014), and unparalleled labeling specificity (Dean & Palmer, 2014), continues to deliver invaluable insight into the fundamental processes that govern living cells in both health and disease. To maximize spatial resolution and detection sensitivity, fluorescence microscopy is traditionally performed with glass coverslips and high-numerical aperture oil immersion objectives.

However, cells are influenced by the molecular composition, mechanical properties, and dimensionality of their environment (Friedl & Wolf, 2009), all of which strongly deviate for optical coverslips from those experienced by cells *in vivo* (Chittajallu *et al.*, 2015). Given these concerns, many in the biological community are moving away from two-dimensional substrates, and instead are now studying biomedically important phenomena within physiological three-dimensional microenvironments (Rubashkin *et al.*, 2014). In particular, many biologists are adopting reconstituted extracellular matrices (Jones *et al.*, 2015) and synthetic scaffolds (Baker *et al.*, 2015), which are more cost-effective, offer greater sample throughput, and are more experimentally tractable than intravital animal imaging.
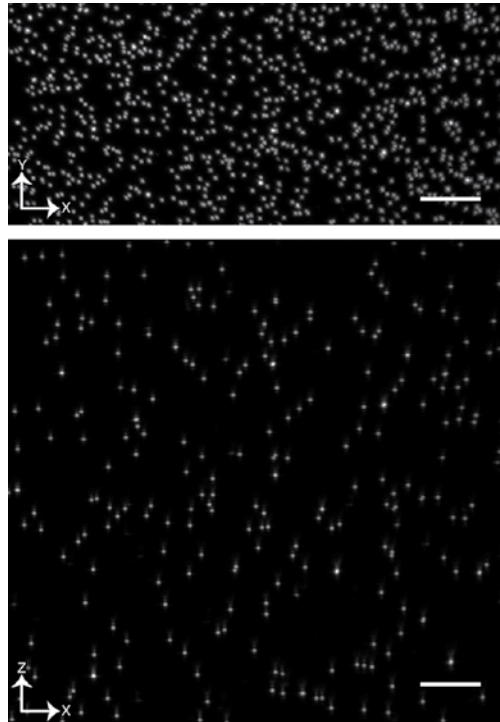
Fig 1: (Top) Lateral and (Bottom) axial view of 200 nm fluorescent beads. Lateral view was obtained by taking a maximum intensity projection (MIP) in the z direction over the whole volume. Axial view was created by taking a MIP over a short distance in the y direction. Scale bar 10 µm.

Fluorescence microscopy is often performed in either a widefield or confocal imaging format. Widefield fluorescence microscopy offers highly parallelized detection, with ~4.2 million pixels in modern scientific cameras, but fails to provide the optical sectioning necessary for imaging in three-dimensional microenvironments (Hiraoka *et al.*, 1990). Here, optical sectioning is defined as the ability to reject fluorescence arising from beyond the focal plane of interest. As such, widefield microscopes suffer from significant out-of-focus image blur, and numerical approaches to eliminate blur (*e.g.,* deconvolution) introduce artifacts and alter the statistical moments of the data (McNally *et al.*, 1999). Indeed, when the shot noise in the out-of-focus signal is comparable to or larger than the in-focus signal, deconvolution algorithms fail to provide satisfactory results. Furthermore, these challenges are worsened in thick samples because

out-of-focus blur accumulates and sample-induced scattering and optical aberrations are unavoidable.

Confocal microscopes operate by imaging the laser focus, and thus the fluorescence arising from it, to a pinhole in the detection path. Fluorescence is measured with a single element photomultiplier tube or an avalanche photodiode (Webb, 1996). Fluorescence outside of the laser focus is predominantly rejected by the pinhole, providing true 3D imaging and optical sectioning in the absence of numerical post-processing. Given that a single-element detector is used, an image is acquired by serially scanning the laser focus through the sample, or the sample through the laser focus, which slows down the rate of image acquisition. When combined with multiphoton excitation, which offers improved optical penetration, confocal microscopy can be performed in the biologically realistic context of a living tissue or animal (Li *et al.*, 2015). However, for any given pixel, the dwell-time of the laser is on the order of a few microseconds, necessitating kW/cm^2 and GW/cm^2 laser intensities for 1- and 2-photon imaging, respectively, that trigger photobleaching and phototoxicity in biological specimens. Decreases in laser intensities can be obtained by parallelizing the illumination with a Nipkow disk, but pinhole cross-talk degrades optical sectioning. Furthermore, whether performed in serial or parallel, pinhole-based detection decreases the photon collection efficiency of an imaging system.

Importantly, in confocal and widefield microscopes, both the in-focus and out-of-focus regions of the cell are both illuminated and fluorescence throughout the sample is inevitably excited. Thus, given the finite number of photons that can be emitted prior to irreversible photobleaching of the fluorophore (Dean *et al.*, 2011), many photons that do not productively contribute to image formation are wasted. To mitigate this, a third technique, referred to as Selective Plane Illumination Microscopy (SPIM), illuminates the sample with a sheet of light, and fluorescence is imaged in an orthogonal
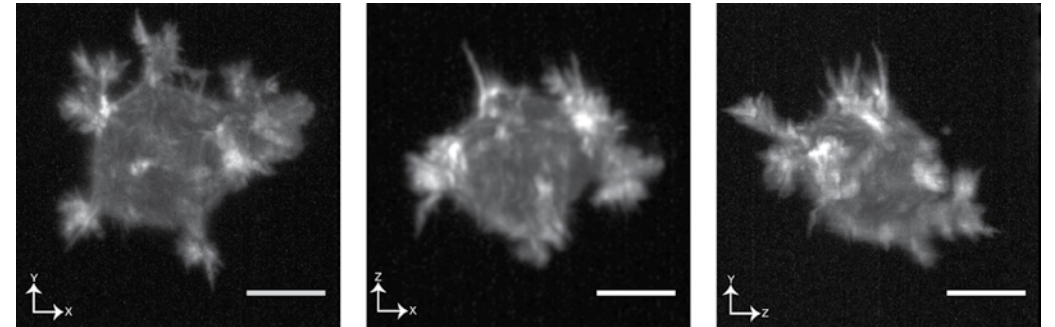

Fig 2: Collagen-embedded human bronchial epithelial cell (HBEC) expressing green fluorescent protein fused to tractin, a protein that binds to the filamentous actin cytoskeleton. Maximum intensity projection along all three spatial orientations are shown. Scale bar 10 µm.

direction on a scientific camera (Huisken *et al.*, 2004). If the illumination beam is sufficiently narrow, only fluorophores located within the depth-of-focus of the detection objective are excited and subsequently detected. As such, out-of-focus illumination is eliminated, all detection objective are excited and subsequently detected (Chhetri *et al.*, 2015). In a SPIM format, 3D volumes are rapidly acquired by scanning the thin sheet of light concurrently with the detection objective (Dean & Fiolka, 2014), or the focal plane of the detection objective (Fahrbach *et al.*, 2013).

One challenge in SPIM is the inverse relationship between image field-of-view and axial resolution, as determined by the illumination beam profile (typically Gaussian) in its propagation direction (~2 Rayleigh lengths) and beam diameter, respectively. Thus to illuminate a large field of view, a beam with a large beam waist has to be used, which results in poor axial resolution. Given this constraint, SPIM has found the greatest use in imaging applications that require moderate axial resolution (~2-4) microns, including whole animal imaging of developing embryos (Keller, 2013). However, much greater resolution is necessary for sub-cellular imaging, and many labs have adopted propagation invariant beams (*e.g.*, Bessel, Airy) in an effort to try to maintain high-resolution imaging throughout larger field of views (Chen et al., 2014, Gao *et al.*, 2012, Planchon *et al.*, 2011, Vettenburg *et al.*, 2014, Fahrbach & Rohrbach, 2012). Nevertheless, in each case, out-of-focus illumination increases with

the size of the field of view, generating image blur that requires deconvolution or multiview image fusion to restore optical sectioning (Wu *et al.*, 2013, Chen et al., 2014, Gao et al., 2012, Planchon et al., 2011). Furthermore, many of these techniques were designed specifically to image thin adherent cells on optical coverslips (Chen et al., 2014, Gao et al., 2012, Planchon *et al.*, 2011). Consequently, no SPIM technique existed that could image cells with isotropic and diffraction-limited resolution throughout large (>100 µm^3) three-dimensional microenvironments.

With these caveats in mind, we developed a SPIM imaging technique, referred to as Axially Swept Light-Sheet Microscopy (ASLM), that enables high-resolution isotropic imaging of cellular processes within large and experimentally tractable 3D microenvironments (Dean *et al.*, 2015). ASLM uses aberration-free remote focusing (Botcherby *et al.*, 2012) to scan a laser line focus (*i.e.*, a narrow sheet of light) in its propagation direction synchronously with a rolling active-pixel array on a scientific CMOS camera (Baumgart & Kubitscheck, 2012). Thereby the camera acquires at any scan position only the waist of the light-sheet, *i.e.*, the portion that yields the sharpest image, and an image with an extended field of view is captured in a single scan. As a result of this unique mechanism, ASLM is capable of simultaneous multicolor imaging of large fields of view (>100 µm^3) with isotropic sub-400 nm resolution and superior optical sectioning strength (Figure 1). For example, ASLM has greater
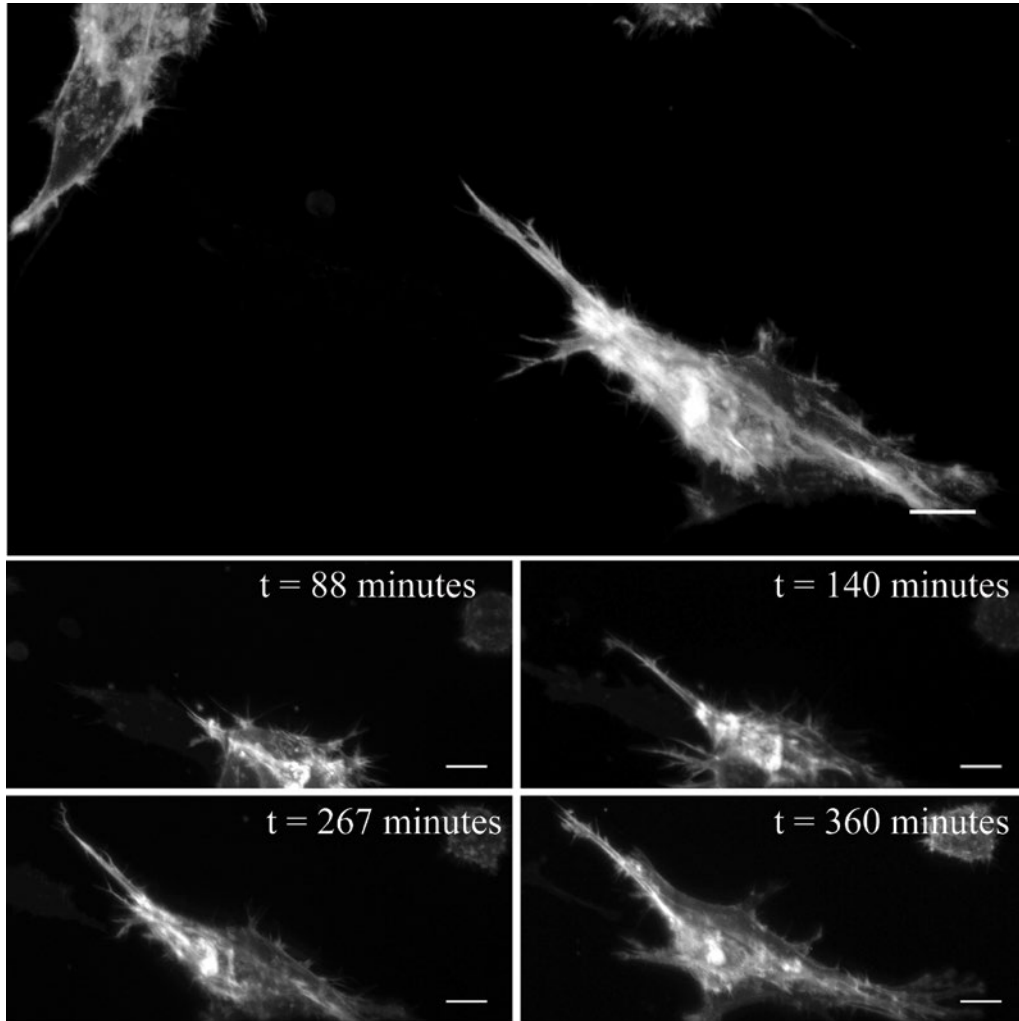
Fig 3: Collagen-embedded retinal pigment epithelial (RPE) expressing green fluorescent protein fused to tractin. (Top) Maximum intensity projection in XY (153x83x100 μm) of multiple RPE cells. (Bottom) Montage of images acquired at different times showing dynamic formation of protrusive lamellipodia-like structures in RPE cells. Scale bar 10 μm.

optical sectioning strength than both 2-photon laser scanning confocal microscopy and 2-photon Bessel-beam SPIM (Planchon *et al.*, 2011). As such, ASLM does not require deconvolution or structured illumination and is uniquely suited for quantitative imaging where precise measurement of intensity ratios (*e.g.*, FRET) of voxel intensities (*e.g.*, single particle tracking) are paramount.

Previously, we used ASLM to image phenotypic heterogeneity in melanoma, mesenchymal cell migration, cell division, and clathrin-mediated endocytosis (Dean *et al.*, 2015). Because of the low-intensity illumination and highly-parallel camera-based detection, cells were routinely imaged for >10 hours and over 2000 z-stacks, enabling the observation of unique cellular behaviors. Here, we present images of polarized human bronchial epithelial cells (Figure 2), lamellipodia-formation in retinal pigment epithelial cells (Figure 3), the distribution of mitochondria in non-polarized retinal pigment epithelial cells (Figure 4), melanoma-collagen interactions (Figure 5), and collective cell migration (Figure 6). Indeed, many of these processes can only be captured at this level of spatial detail with ASLM's uncompromised resolution, field of view, and optical sectioning, making ASLM uniquely qualified to study cell biology in three-dimensional microenvironments.

Biographies:

Kevin Dean is a postdoctoral fellow in Gaudenz Danuser's lab at UT Southwestern Medical Center in Dallas, Texas. He was raised in Northern California, received his B.A. in Chemistry at Willamette University, and completed his Ph.D. in Biochemistry at the University of Colorado. Under the guidance of Prof. Amy Palmer, his doctoral work focused on fluorescent protein spectroscopy and engineering with high-throughput multiparameter microfluidic cell sorters. Following graduation, he served as the Director of the BioFrontiers Advanced Imaging Resource. Today, his research aims to integrate advanced light-sheet microscopy, computer vision, and cell biology to understand cytoskeletal dynamics and signal transduction in 3D extracellular matrix environments.

Reto Fiolka is an instructor in the Department of Cell Biology at UT Southwestern. He was born in Switzerland and studied Mechanical Engineering at ETH Zurich, where he also completed his PhD in advanced microscopy techniques involving structured illumination and diffraction tomography. He performed postdoctoral research at HHMI's Janelia Farm research campus under the guidance of the late Mats Gustafsson on the development of live 3D structured illumination microscopy. In a second postdoctoral stay at Janelia Farm, he worked with
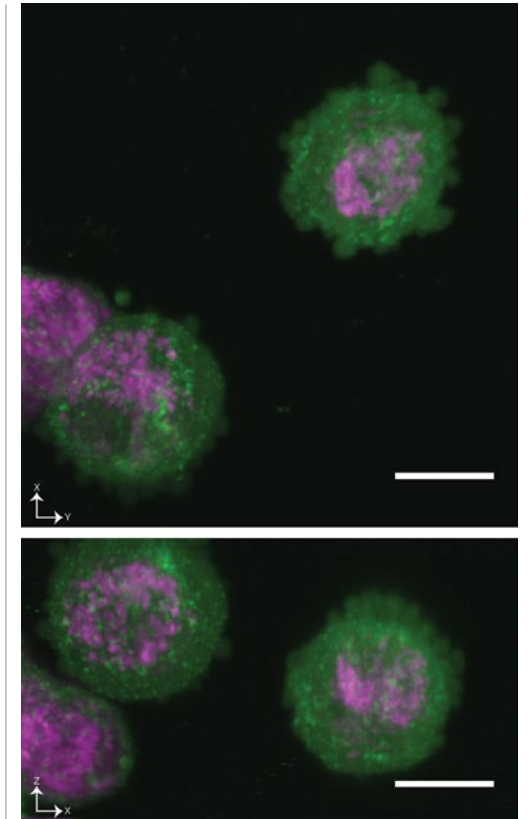

Fig 4: ARPE19 cells (retinal pigment epithelial cells from another source) labeled with clathrin light chain alpha (CLCa) green fluorescent protein (shown in green) and MitoTracker orange (shown in magenta). CLCa marks sites of clathrin-mediated endocytosis and internal clathrin-positive structures (e.g., the Golgi apparatus). MitoTracker is a cell-permeable fluorophore that labels mitochondria. Both a lateral and an axial view of the volume are shown. Scale bar 10 μm.

Meng Cui on adaptive optics. At UT Southwestern, Reto Fiolka now develops imaging technologies for imaging cells in 3D microenvironments with high spatiotemporal resolution.

References:

Ahrens, M. B., Orger, M. B., Robson, D. N., Li, J. M. & Keller, P. J. (2013) Whole-brain functional imaging at cellular resolution using light-sheet microscopy. *Nature Methods,* **10,** 413-420.

Baker, B. M., Trappmann, B., Wang, W. Y., Sakar, M. S., Kim, I. L., Shenoy, V. B., Burdick, J. A. & Chen, C. S. (2015) Cell-mediated fibre recruitment drives extracellular matrix mechanosensing in engineered fibrillar microenvironments. *Nature Materials*.

Baumgart, E. & Kubitscheck, U. (2012) Scanned light sheet microscopy with confocal slit detection. *Opt*

Express, **20,** 21805-21814.

Botcherby, E. J., Smith, C. W., Kohl, M. M., Debarre, D., Booth, M. J., Juskaitis, R., Paulsen, O. & Wilson, T. (2012) Aberration-free three-dimensional multiphoton imaging of neuronal activity at kHz rates. *Proceedings of the National Academy of Sciences,* **109,** 2919-2924.

Chen, B. C., Legant, W. R., Wang, K., Shao, L., Milkie, D. E., Davidson, M. W., Janetopoulos, C., Wu, X. S., Hammer, J. A., Liu, Z., English, B. P., Mimori-Kiyosue, Y., Romero, D. P., Ritter, A. T., Lippincott-Schwartz, J., Fritz-Laylin, L., Mullins, R. D., Mitchell, D. M., Bembenek, J. N., Reymann, A. C., Bohme, R., Grill, S. W., Wang, J. T., Seydoux, G., Tulu, U. S., Kiehart, D. P. & Betzig, E. (2014) Lattice light-sheet microscopy: Imaging molecules to embryos at high spatiotemporal resolution. *Science,* **346,** 1257998-1257998.

Chhetri, R. K., Amat, F., Wan, Y., Höckendorf, B., Lemon, W. C. & Keller, P. J. (2015) Whole-animal functional and developmental imaging with isotropic spatial resolution. *Nature Methods.*

Chittajallu, D. R., Florian, S., Kohler, R. H., Iwamoto, Y., Orth, J. D., Weissleder, R., Danuser, G. & Mitchison, T. J. (2015) In vivo cell-cycle profiling in xenograft tumors by quantitative intravital microscopy. *Nature Methods,* **12,** 577-585.

Dean, K. M. & Fiolka, R. (2014) Uniform and scalable light-sheets generated by extended focusing. *Optics Express,* **22,** 26141.

Dean, Kevin M., Lubbeck, Jennifer L., Binder, Jennifer K., Schwall, Linda R., Jimenez, R. & Palmer, Amy E. (2011) Analysis of Red-Fluorescent Proteins Provides Insight into Dark-State Conversion and Photodegradation. *Biophysical Journal,* **101,** 961-969.

Dean, K. M. & Palmer, A. E. (2014) Advances in fluorescence labeling strategies for dynamic cellular imaging. *Nature Chemical Biology,* **10,** 512-523.

Dean, Kevin M., Roudot, P., Welf, Erik S., Danuser, G. & Fiolka, R. (2015) Deconvolution-free Subcellular Imaging with Axially Swept Light Sheet Microscopy. *Biophysical Journal,* **108,** 2807-2815.

Fahrbach, F. O. & Rohrbach, A. (2012) Propagation stability of self-reconstructing Bessel beams enables contrast-enhanced imaging in thick media. *Nat Commun,* **3,** 632.

Fahrbach, F. O., Voigt, F. F., Schmid, B., Helmchen, F. & Huisken, J. (2013) Rapid 3D light-sheet microscopy with a tunable lens. *Optics Express,* **21,** 21010.

Friedl, P. & Wolf, K. (2009) Plasticity of cell migration: a multiscale tuning model. *The Journal of Cell Biology,* **188,** 11-19.

Gao, L., Shao, L., Higgins, Christopher D., Poulton, John S., Peifer, M., Davidson, Michael W., Wu, X., Goldstein, B. & Betzig, E. (2012) Noninvasive Imaging beyond the Diffraction Limit of 3D Dynamics in
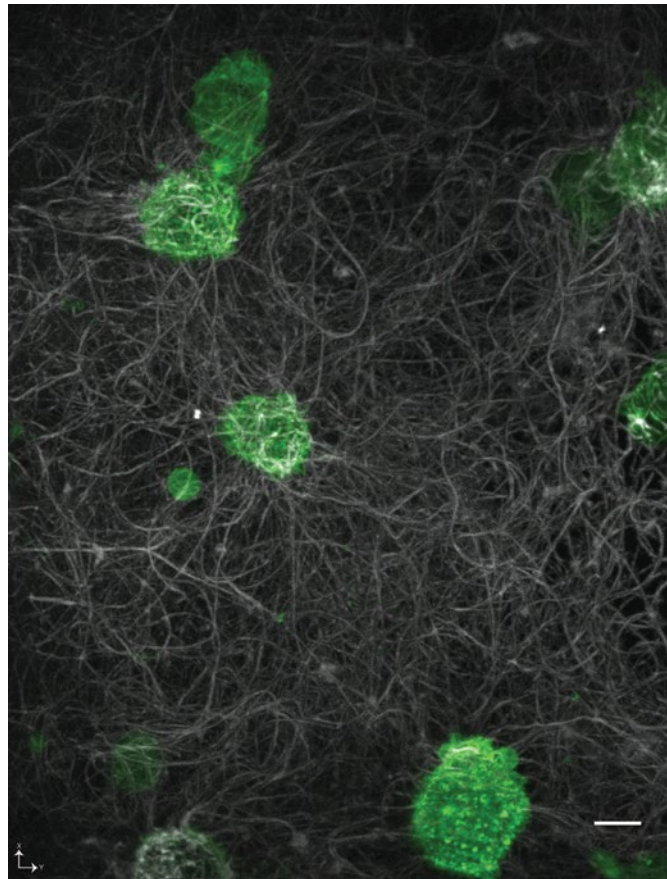
Fig 5: Maximum intensity projection in XY of MV3 melanoma cells expressing green fluorescent protein fused to tractin, embedded in a fluorescently-labeled collagen matrix. Image dimension is 184x140x100 µm, in X, Y, and Z, respectively. Scale bar 10 µm.
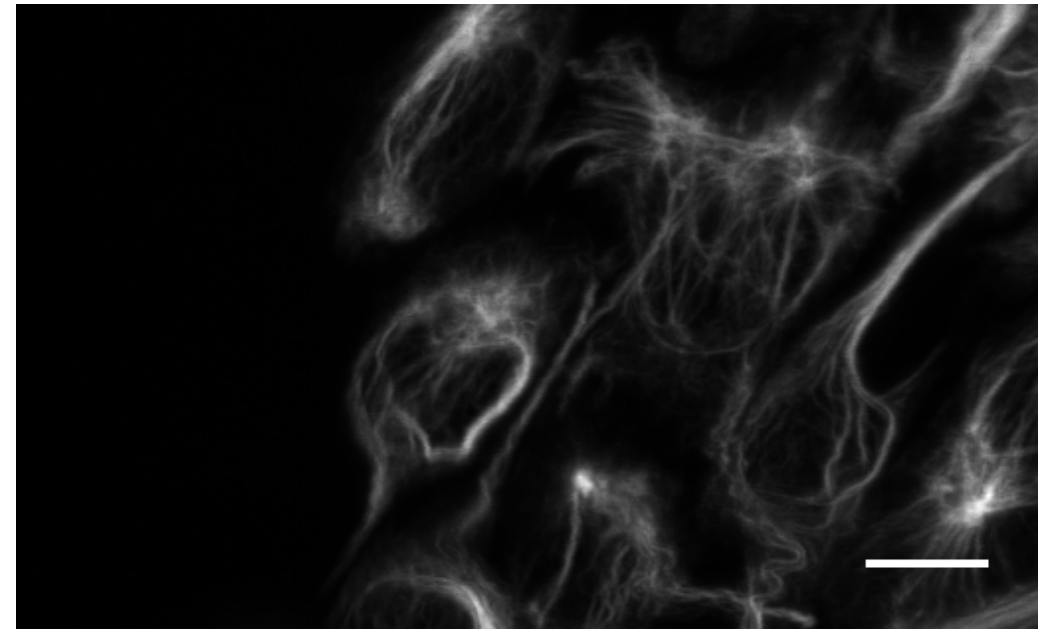

Fig 6: Maximum intensity projection in XZ of RPE cells undergoing collective migration in a wound healing assay. Cells were genome modified expressed vimentin fused to green fluorescent protein from its native chromosomal loci in a heterozygous fashion. Scale bar 10 µm.

Thickly Fluorescent Specimens. *Cell,* **151,** 1370-1385.

Hiraoka, Y., Sedat, J. W. & Agard, D. A. (1990) Determination of three-dimensional imaging properties of a light microscope system. Partial confocal behavior in epifluorescence microscopy. *Biophysical Journal,* **57,** 325-333.

Huisken, J., Swoger, J., Del Bene, F., Wittbrodt, J. & Stelzer, E. H. (2004) Optical sectioning deep inside live embryos by selective plane illumination microscopy. *Science,* **305,** 1007-1009.

Jones, C. A. R., Cibula, M., Feng, J., Krnacik, E. A., McIntyre, D. H., Levine, H. & Sun, B. (2015) Micromechanics of cellularized biopolymer networks. *Proceedings of the National Academy of Sciences,* **112,** E5117-E5122.

Keller, P. J. (2013) Imaging Morphogenesis: Technological Advances and Biological Insights. *Science,* **340,** 1234168-1234168.

Li, N., Chen, T.-W., Guo, Z. V., Gerfen, C. R. & Svoboda, K. (2015) A motor cortex circuit for motor planning and movement. *Nature,* **519,** 51-56.

McNally, J. G., Karpova, T., Cooper, J. & Conchello, J. A. (1999) Three-Dimensional Imaging by Deconvolution Microscopy. *Methods,* **19,** 373-385.

Planchon, T. A., Gao, L., Milkie, D. E., Davidson, M. W., Galbraith, J. A., Galbraith, C. G. & Betzig, E. (2011)

Rapid three-dimensional isotropic imaging of living cells using Bessel beam plane illumination. *Nature Methods,* **8,** 417-423.

Rubashkin, M. G., Ou, G. & Weaver, V. M. (2014) Deconstructing Signaling in Three Dimensions. *Biochemistry,* **53,** 2078-2090.

Van Engelenburg, S. B., Shtengel, G., Sengupta, P., Waki, K., Jarnik, M., Ablan, S. D., Freed, E. O., Hess, H. F. & Lippincott-Schwartz, J. (2014) Distribution of ESCRT Machinery at HIV Assembly Sites Reveals Virus Scaffolding of ESCRT Subunits. *Science,* **343,** 653-656.

Vettenburg, T., Dalgarno, H. I. C., Nylk, J., Coll-Lladó, C., Ferrier, D. E. K., □ižmár, T., Gunn-Moore, F. J. & Dholakia, K. (2014) Light-sheet microscopy using an Airy beam. *Nature Methods,* **11,** 541-544.

Webb, R. H. (1996) Confocal optical microscopy. *Reports on Progress in Physics,* **59,** 427-471.

Wu, Y., Wawrzusin, P., Senseney, J., Fischer, R. S., Christensen, R., Santella, A., York, A. G., Winter, P. W., Waterman, C. M., Bao, Z., Colón-Ramos, D. A., McAuliffe, M. & Shroff, H. (2013) Spatially isotropic four-dimensional imaging with dual-view plane illumination microscopy. *Nature Biotechnology,* **31,** 1032-1038.